JOURNAL OF PROPULSION AND POWER
Vol. 25, No. 3, May–June 2009

Technical Notes

TECHNICAL NOTES are short manuscripts describing new developments or important results of a preliminary nature. These Notes should not exceed 2500 words (where a figure or table counts as 200 words). Following informal review by the Editors, they may be published within a few months of the date of receipt. Style requirements are the same as for regular contributions (see inside back cover).

Development of a Specific Impulse Balance for Capillary Discharge Pulsed Plasma Thrusters

T. C. Lilly* and A. D. Ketsdever†
University of Colorado, Colorado Springs, Colorado 80933
A. P. Pancotti‡
ERC Incorporated, Edwards Air Force Base, California 93524
and
M. Young§
Air Force Research Laboratory, Edwards Air Force Base, California 93524

DOI: 10.2514/1.40261

I. Introduction

CAPILLARY-DISCHARGE-BASED (CD), coaxial, electrothermal pulsed plasma thrusters (PPT) are currently under development as a high-efficiency alternative to more traditional ablative PPTs. The major drawback of the traditional ablative PPT is the propulsive efficiency. Even though specific impulses (I_{sp}) on the order of 1000 s have been achieved with ablative PPTs using electromagnetic acceleration, the propulsive efficiencies of flight-qualified thrusters typically remains below 10% [1]. Capillary discharges are relatively efficient sources of high-density, high-temperature plasmas, which are being developed for a number of applications [2–4]. The CD operates on a solid propellant ablated from a relatively long tube during a pulsed discharge. Previous performance calculations have suggested that a capillary-discharge-based electrothermal PPT can achieve propulsive efficiencies of 30–40% even without nozzle expansion [5]. Additional studies indicate that nozzle expansion of the high-pressure, high-temperature plasma generated by the capillary discharge will increase the efficiency above 50% [6]. With the potential for vast improvement in efficiency, the capillary-discharge, electrothermal PPT may be a strong candidate for satellite attitude control and station-keeping maneuvers.

In the present study, a diagnostic tool has been developed to investigate the applicability of a capillary discharge as an electrothermal PPT. A torsion thrust stand similar to that described in [7] has been designed and built to simultaneously measure the impulse and mass loss of the capillary discharge. The simultaneous nature of the developed technique will allow a per-pulse measurement of the discharge's specific impulse through the relation

$$I_{sp} = \frac{I_{tot}}{m_{prop} g_0} \tag{1}$$

where I_{tot} is the total impulse, m_{prop} is the total propellant mass loss, and g_0 is the gravitational constant. The thruster will be configured on the thrust stand such that the impulse generated by the discharge and the steady-state force generated by the propellant mass loss act in the same direction. The combined signal from these effects can then be decoupled to assess the ratio of the impulse to the weight of propellant expended, yielding the specific impulse.

The thrust stand system developed in [7] has several advantages over more traditional methods of measuring specific impulse in solid propellant thrusters. First, the amount of mass loss is relatively low when compared with the associated impulse provided by a high-I_{sp} thruster. Traditional mass loss measurements would require the averaging of multiple thruster firings to obtain meaningful data. By developing a system capable of measuring signals over several orders of magnitude, impulse and mass loss measurements can be made simultaneously on a shot-to-shot basis. Second, the system mass is traditionally measured before the performance measurements, and again after, to assess the propellant mass used [8]. These measurements may take place days apart and may require the system to be placed into a vacuum chamber and subsequently removed in between thruster firings at the cost of valuable time and resources. Finally, issues of handling, contamination, oxidation, and adsorption may complicate mass measurements that are not done in situ.

The simultaneous measurement of the total impulse and propellant mass loss is discussed in detail in [7]. In short, the thrust stand acts as an over-damped second-order oscillator whose motion in response to a known forcing moment can be predicted by its moment of inertia (I), damping coefficient (C), and torsion spring constant (K). For impulses with pulse widths much shorter than the period of the thrust stand, the magnitude of the total impulse imparted to the stand has a linear relation with the maximum deflection range of its motion. The mass loss has an equally well-defined relation to the difference between the initial zero position of the thrust stand and the final position once oscillatory motion has sufficiently damped. Examples of these relations can be seen in Figs. 1 and 2. Note that a thrust stand for a given application can be designed such that the range (governed by I, C, and K) is much larger than the steady-state deflection (governed only by K), thereby minimizing the error in the impulse measurement due to the steady-state mass loss. Using the model derived and validated in [9], the configuration of an operational thrust stand will be discussed in following sections.

II. Thrust Stand Design

The major components of the thrust stand are the rotational arm, damping magnets, flexure pivots (torsion springs), displacement sensor, and calibration system. The rotational arm contributes to the moment of inertia I of the stand and provides a structure to attach the thruster and other components. The damping magnets are used as eddy current generators to damp the stand's motion and define the

Presented as Paper 4740 at the 44th AIAA/ASME/SAE/ASEE Joint Propulsion Conference & Exhibit, Hartford, CT, 21–23 July 2008; received 5 August 2008; revision received 11 November 2008; accepted for publication 22 December 2008. Copyright © 2008 by the American Institute of Aeronautics and Astronautics, Inc. All rights reserved. Copies of this paper may be made for personal or internal use, on condition that the copier pay the $10.00 per-copy fee to the Copyright Clearance Center, Inc., 222 Rosewood Drive, Danvers, MA 01923; include the code 0748-4658/09 $10.00 in correspondence with the CCC.

*Senior Professional Research Assistant, 1420 Austin Bluffs Parkway, University Hall Room 231. Student Member AIAA.
†Assistant Professor of Mechanical and Aerospace Engineering, 1420 Austin Bluffs Parkway UH231. Associate Fellow AIAA.
‡Research Engineer, 10 East Saturn Boulevard. Student Member AIAA.
§Deputy Program Manager of Advanced Concepts, Propulsion Directorate, 10 East Saturn Boulevard. Member AIAA.

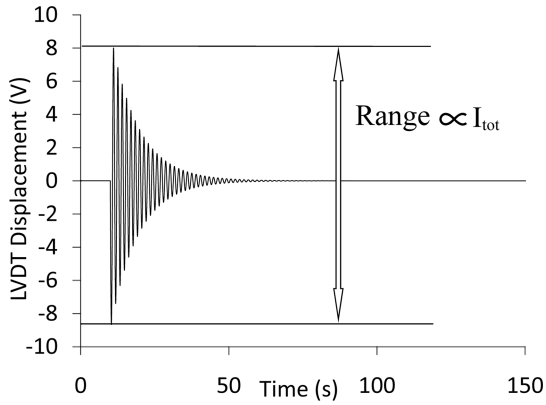

Fig. 1 Simulated LVDT reading for expected impulse from an operational capillary discharge.

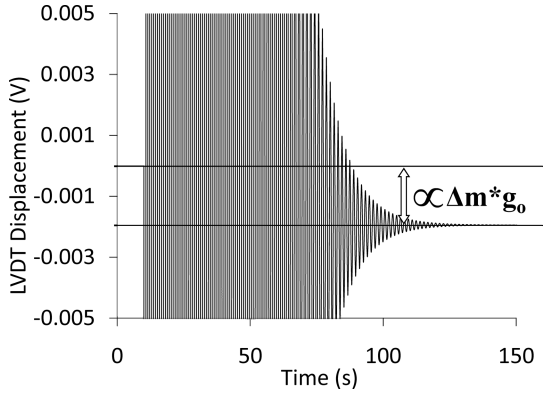

Fig. 2 Simulated LVDT reading for expected mass loss from an operational capillary discharge.

damping coefficient C of the stand. The torsion springs (flexures) contribute to the spring constant K by providing the restoring force for the stand. The displacement sensor measures the linear motion of the stand and defines the limits of the stand's motion as well as the precision of the measurements. The calibration system provides a known steady-state force or transient impulse to the stand and defines the useful range of the stand's accuracy. The major components of a thrust stand can be seen in Fig. 3.

Special consideration must be given to a choice in displacement sensors because the CD involves strong electromagnetic fields during the discharge. Such fields will interfere with any locally mounted electronic force sensors, such as piezo-based load cells. This interference is only present during the thruster firing, for which the thrust stand has an advantage. The pertinent measurement of the thrust stand's motion required for an impulse determination is made relatively long after the thruster firing. Thus, for sensors that recover from the electromagnetic interference sufficiently quick, the effect from the interference is negligible. Linear variable differential transformers (LVDTs) have been successfully implemented on a previous thrust stand [7]. These sensors have an advertised repeatability less than or equal to 0.01%. The useful range and accuracy of the detector, for a given thrust stand configuration, directly sets the maximum impulse and minimum mass loss able to be resolved by the thrust stand.

To correlate position measurements with known forces and impulses, the stand must be calibrated in the same configuration that the thruster testing is conducted. The most straightforward system of calibration is to place calibrated weights on the stand to create a known force. Unfortunately, this method is not easily replicated for in situ vacuum calibration or short-duration impulses. Previous iterations of thrust stands have used electrostatic combs to generate repeatable and known attractive forces [10]. To cover the lower region of impulse calibration and allow for steady-state force calibration, a larger-scale electrostatic calibration system has been designed and built to impart up to a 5×10^{-2} N force to the thrust stand. To cover the higher region of impulse calibration, a piezoelectric impact hammer will be implemented to calibrate in the $10^{-4} - 10^{1}$ N · s range. Figure 4 shows the linear relationship obtained between the impact hammer impulse and the deflection range of the thrust stand.

When choosing a set of flexures for the stand, the primary concern for the specific impulse measurement is that the change in beginning and ending positions due to CD mass loss is large enough to be resolved by the displacement sensor and ancillary acquisition hardware, yet small enough not to cause a large error in the impulse measurement. For the steady-state condition before and after the CD discharge, the displacement of the thrust stand is only dependant on the magnitude and position of the mass loss and the spring constant K of the stand. Figure 5 shows the expected LVDT reading for a 12 mg mass loss, the amount predicted by the CD model in [6], as measured

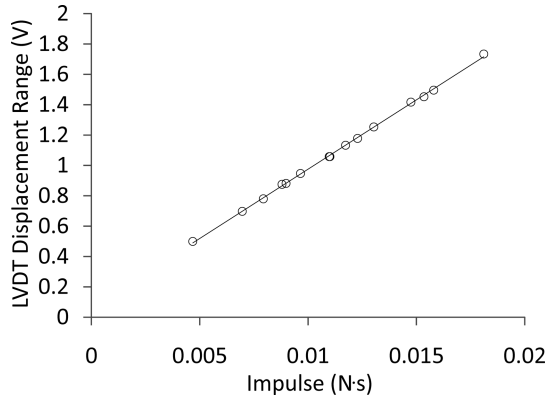

Fig. 4 Thrust stand deflection range vs imparted impulse from an impact hammer ($R^2 = 0.9993$).

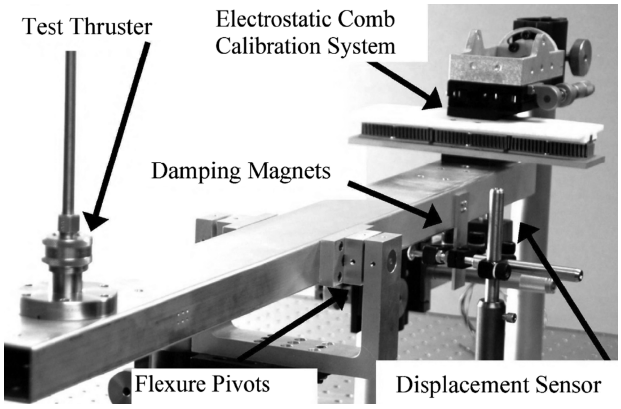

Fig. 3 Major thrust stand components.

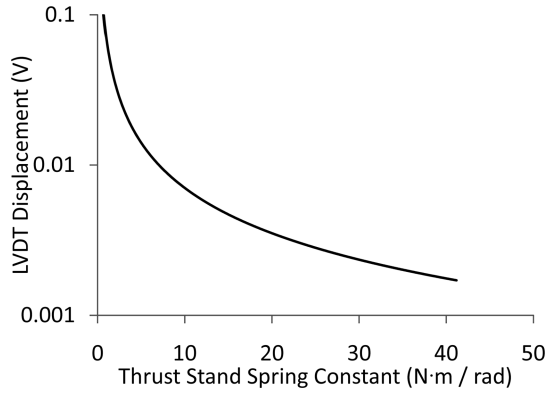

Fig. 5 Thrust stand deflection vs spring constant K.

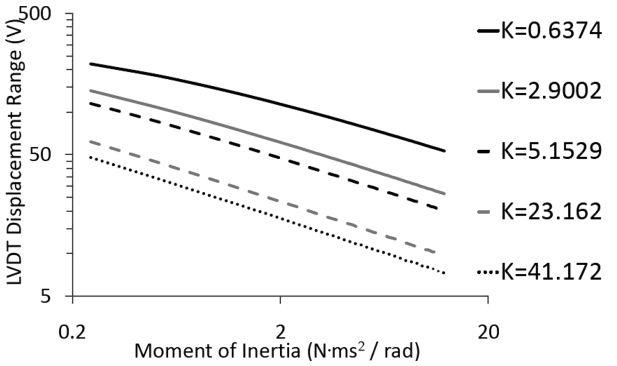

Fig. 6 Thrust stand deflection range vs *I* for multiple *K* (note logarithmic axes).

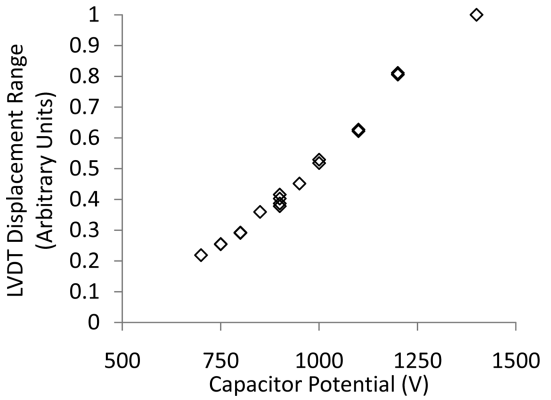

Fig. 7 Thrust stand displacement range vs CD capacitor potential.

by the designed thrust stand as a function of the spring constant. Given a data acquisition hardware resolution of better than 1 mV, a thrust stand using any of the spring constants in the plotted range would be able to resolve a single-shot mass loss measurement. For high resolution, the preference for larger displacements can be obtained for smaller values of the spring constant. The spring constant, as well as the moment of inertia, affects the maximum range of the thrust stand for a given impulse. The range decreases with increasing spring constant and moment of inertia, as seen in Fig. 6. There is a diminishing return for limiting the range by increasing the moment of inertia of the thrust stand; therefore, the inherent limit of the displacement sensor indicates that higher spring constants are needed to limit the range produced by a given applied impulse. This leads to a trade that yields an optimum value for the spring constant when balancing between the sensitivity needed for the mass loss measurements and the restoring force needed for the total impulse measurements.

III. Results and Discussion

As an iterative first step to CD-specific impulse measurements, a thrust stand comprising only the major elements was built. This iteration was used to validate the thrust stand model in [9] and its use for this application. It was also used as a test bed for integrating the thruster, calibration, and sensing equipment. The model coefficients for the first-iteration thrust stand can be seen in Table 1. The measured *K* value matches the advertised unloaded spring constant from the manufacturer (published as $\pm 10\%$) within 1.5%. The measured motion of the thrust stand matched the model predicted motion. To test the CD attachment, data acquisition and control, power transfer connections, and feasibility of using an LVDT in the vicinity of the discharge, the CD was attached to the first-iteration thrust stand. Because the first-iteration thrust stand was not designed for the CD at operational power levels, the CD was operated at relatively low power. The displacement range measured by the LVDT on this stand vs the voltage potential on the discharge capacitor bank can be seen in Fig. 7. From [6], the total impulse should increase with an increase in capacitor potential, a trend that is reflected by the increase in measured deflection range.

With an experimentally validated model, the design space for the modification of the thrust stand for measuring the expected CD performance values from [6] was investigated. This trade study consisted of running the model for a variety of flexures and moments of inertia shown in Fig. 6. The first-iteration thrust stand could not measure the operational capillary discharge impulse as it would result in a range larger than the linear section of the LVDT. From Fig. 6, it is possible to limit this range of motion by increasing the spring constant of the stand; however, too large a *K* value would not allow the stand to be useful for accurate mass loss measurements. Altering the moment of inertia offers near continuous values of the range simply by adding mass to the rotational arm without degrading resolution in the mass loss measurements.

Based on estimates from the preformed trade study, the first-iteration stand's moment of inertia was modified by adding 5 kg to the end of each side of the rotational arm. In addition, the original aluminum damping plate was replaced with a copper plate, which generated a larger damping force to reduce stand motion. These changes can be seen in Fig. 8 and the characteristics of the stand in Table 1. After modifications, the model and modified stand were tested. The change in *I* and observed change in *K* are properly reflected in a change in measured period and maximum deflection

Table 1 Thrust stand characteristics

Thrust stand	First iteration	Operational
K, N m/rad	41.75	36.22
C, N m s/rad	0.191	0.428
I, N m s^2/rad	0.245	1.988

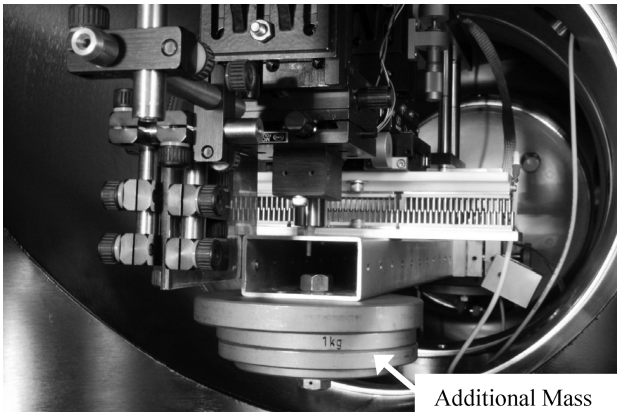

Fig. 8 Experimental thrust stand, calibration system, LVDT, and magnetic damping.

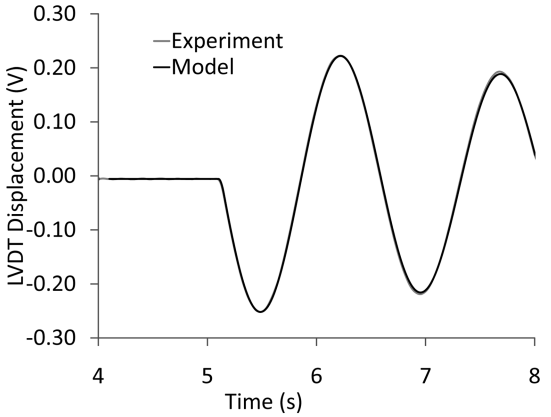

Fig. 9 Model comparison for the operational thrust stand for a 3.63 mN · s impulse.

range between the two iterations. The comparison between the operational (modified) thrust stand and the model used for the trade study can be seen in Fig. 9. (Note that the experimental line and the model line nearly overlap.)

While operating at its full discharge potential, the CD is expected to produce approximately 10^{-1} N · s impulse with a propellant mass loss of 12 mg [6]. The expected output of the LVDT for such a firing on the operational thrust stand can be seen in Figs. 1 and 2. This represents the operational levels for which the thrust stand was designed and modified. If experimental values are found to be significantly different than those predicted by the CD model, the thrust stand maintains the flexibility to be easily reconfigured for a large range of total impulse and propellant mass loss values by variations in the mass moment of inertia, spring constant and/or damping coefficient.

Acknowledgments

This work was supported by the Advanced Concepts Group at the Propulsion Directorate of the U.S. Air Force Research Laboratory at Edwards Air Force Base.

References

[1] Kamhawi, H., Arrington, L., Pencil, E., and Haag, T., "Performance Evaluation of a High Energy Density Pulsed Plasma Thruster," AIAA Paper 2005-3695, 2005.

[2] Zigler, A., Ehrlich, Y., Cohen, C., Krall, J., and Sprangle, P., "Optical Guiding of High-Intensity Laser Pulsed in a Long Plasma Channel Formed by a Slow Capillary Discharge," *Journal of the Optical Society of America B (Optical Physics)*, Vol. 13, 1996, pp. 68–71. doi:10.1364/JOSAB.13.000068

[3] Lee, R., and Zigler, A., "Multiple Pulse Laser Excitation of a Capillary Discharge," *Applied Physics Letters*, Vol. 53, No. 21, 1988, pp. 2028–2029. doi:10.1063/1.100311

[4] Powell, J., and Zielinski, A., "Theory and Experiment for an Ablating Capillary Discharge and Application to Electrothermal-Chemical Guns," U.S. Army Ballistic Research Lab., Rept. BRL-TR-3355, Aberdeen Proving Ground, MD, June 1992.

[5] Cambier, J., Young, M., Pekker, L., and Pancotti, A., "Capillary Discharge Based Pulsed Plasma Thrusters," *International Electric Propulsion Conference*, Electric Rocket Propulsion Society, Fairview Park, OH, Paper 2007-238, 2007.

[6] Pekker, L., and Cambier, J., "A Model of Ablative Capillary Discharge," Assembly for International Heat Transfer, IHTC-13, Aug. 2006.

[7] Ketsdever, A., Lee, R., and D'Souza, B., "Thrust Stand Micro-Mass Balance for the Direct Measurement of Specific Impulse," *Journal of Propulsion and Power*, Vol. 24, No. 6, 2008, pp. 1376–1381.doi: 10.2514/1.36921

[8] Fredrick, R. A., and Greiner, B. E., "Laboratory-Scale Hybrid Rocket Motor Uncertainty," *Journal of Propulsion and Power*, Vol. 12, No. 3, 1996, pp. 605–611. doi:10.2514/3.24076

[9] D'Souza, B., and Ketsdever, A., "Investigation of Time-Dependent Forces on a Nano-Newton-Second Impulse Balance," *Review of Scientific Instruments*, Vol. 76, No. 1, 2005, pp. 015105–015105-10.doi:10.1063/1.1834707

[10] Selden, N. P., and Ketsdever, A. D., "Comparison of Force Balance Calibration Techniques for the Nano-Newton Range," *Review of Scientific Instruments*, Vol. 74, No. 12, 2003, pp. 5249–54.doi: 10.1063/1.1623628

C. Segal
Associate Editor